Experimental Hematology

Experimental Hematology 2016;44:161–165

BRIEF COMMUNICATIONS

Deletion of *Rb1* induces both hyperproliferation and cell death in murine germinal center B cells

Zhiwen He[a], Julie O'Neal[a], William C. Wilson[a], Nitin Mahajan[a], Jun Luo[a], Yinan Wang[b], Mack Y. Su[a], Lan Lu[a], James B. Skeath[c], Deepta Bhattacharya[b], and Michael H. Tomasson[a]

[a]*Department of Internal Medicine, Division of Oncology, Washington University School of Medicine, St. Louis, MO;* [b]*Department of Pathology and Immunology, Washington University School of Medicine, St. Louis, MO;* [c]*Department of Genetics, Washington University School of Medicine, St. Louis, MO*

(Received 15 August 2014; revised 21 September 2015; accepted 7 November 2015)

The retinoblastoma gene (*RB1*) has been implicated as a tumor suppressor in multiple myeloma (MM), yet its role remains unclear because in the majority of cases with 13q14 deletions, un-mutated *RB1* remains expressed from the retained allele. To explore the role of *Rb1* in MM, we examined the functional consequences of single- and double-copy *Rb1* loss in germinal center B cells, the cells of origin of MM. We generated mice without *Rb1* function in germinal center B cells by crossing $Rb1^{Flox/Flox}$ with C-γ-1-Cre (Cγ1) mice expressing the Cre recombinase in class-switched B cells in a $p107^{-/-}$ background to prevent *p107* from compensating for *Rb1* loss ($C\gamma1\text{-}Rb1^{F/F}\text{-}p107^{-/-}$). All mice developed normally, but B cells with two copies of *Rb1* deleted ($C\gamma1\text{-}Rb1^{F/F}\text{-}p107^{-/-}$) exhibited increased proliferation and cell death compared with $C\gamma1\text{-}Rb1^{+/+}\text{-}p107^{-/-}$ controls ex vivo. In vivo, $C\gamma1\text{-}Rb1^{F/F}\text{-}p107^{-/-}$ mice had a lower percentage of splenic B220+ cells and reduced numbers of bone marrow antigen-specific secreting cells compared with control mice. Our data indicate that Rb1 loss induces both cell proliferation and death in germinal center B cells. Because no B-cell malignancies developed after 1 year of observation, our data also suggest that *Rb1* loss is not sufficient to transform post-germinal center B cells and that additional, specific mutations are likely required to cooperate with *Rb1* loss to induce malignant transformation.

Large deletions affecting chromosome 13 occur in 50% of cases of multiple myeloma (MM) and are associated with poor long-term survival [1]. The role of chromosome 13 deletions in MM has been the focus of intense study, but the tumor suppressor gene(s) has not been conclusively identified [2]. The retinoblastoma (*RB1*) gene has been implicated as a candidate tumor suppressor at 13q14 in MM [3]. Previously, we mapped chromosome 13 deletions in MM and found a microdeletion in a t(4;14)-positive patient that removed a single exon of *RB1* critical for its function [4]. High-resolution genetic studies, including single-nucleotide polymorphism (SNP) array studies [5] and whole-genome sequencing approaches [6,7], have also found that *RB1* is a recurrent deletion target in MM. Of note though, retained *RB1* alleles remain un-mutated and expressed in the majority of cases of MM [8]. *RB1* is the gene that defined bi-allelic loss as the sine qua non of tumor suppressor gene function [9], however, given the frequent mono-allelic loss of *RB1* and the central role of *Cyclin D/Rb* pathway in MM, if *RB1* is the target of chromosome

ZH and JO contributed equally to this work.

Offprint requests to: Michael H. Tomasson, Department of Internal Medicine, Washington University School of Medicine, 660 South Euclid, Campus Box 8069, St. Louis, MO 63110; E-mail: tomasson@dom.wustl.edu

Supplementary data related to this article can be found online at http://dx.doi.org/10.1016/j.exphem.2015.11.006.

http://dx.doi.org/10.1016/j.exphem.2015.11.006

13 deletion, it remains an enigma why it is infrequently biallelically inactivated [10].

The function of *Rb1* as a tumor suppressor has been well studied, and genetically targeted mice have been invaluable tools in dissecting the role of *Rb1* in tumor development [11,12]. Germline deletion of *Rb1* is embryonic-lethal with defects in neurogenesis and hematopoiesis [2,13,14]. Mice engineered with a conditional *Rb1* allele develop pituitary tumors, illustrating the tumor-suppressor activity of *Rb1* [15,16]. However, mice with conditional loss of *Rb1* do not develop retinoblastoma tumors as was expected from human genetic studies. In mice, two additional *Rb* family members, *p107* and *p130*, have redundant tumor suppressor function [17–20], thus complicating the study of the role of *Rb1* in tumorigenesis. The *p107* family member is upregulated on *Rb1* loss in the mouse retina, and deletion of *p107* is necessary before retinoblastoma tumors develop [19].

To identify potential roles of *Rb1* in MM pathogenesis, we generated triple transgenic mice with conditional deletion of *Rb1* in germinal center (GC) B cells. We observed increased proliferation in *Rb1* null B cells stimulated to undergo class-switch recombination (CSR). In vivo, mice with *Rb1* deleted in GC B cells had a smaller percentage of splenic B220+ cells and fewer bone marrow antigen-specific secreting cells (ASCs) compared with control mice. Our data suggest that complete absence of *Rb1* in antigen-stimulated cells results in hyperproliferation balanced by cell death.

Methods

Detailed methods are described in the Supplementary Material (online only, available at www.exphem.org).

Results and discussion

We sought to generate strains of mice with *Rb1* function deleted from GC B cells. The *Rb1* family members *Rbl1 (p107)* and *Rbl2 (p130)* compensate for *Rb1* loss in some cell types [19], so we examined the transcript expression of all three retinoblastoma family genes at four stages of B-cell development: naive B, GC B, plasma B, and memory B cells [21]. We found that *Rb1* and *p107*, but not *p130*, were expressed in mature B-cell subsets including GC and plasma cells (Fig. 1A). These data suggested that *p107* might compensate for *Rb1* loss in GC cells, so we generated triple transgenic mice using the previously characterized conditional $Rb1^{Flox}$ allele, Cγ1-cre, which expresses cre recombinase specifically in GC B cells [22], and a *p107* null allele. In this way, we established three strains of mice: Cγ1-$Rb1^{F/F}$-$p107^{-/-}$, Cγ1-$Rb1^{F/+}$-$p107^{-/-}$, and Cγ1-$Rb1^{+/+}$-$p107^{-/-}$ (which will be referred to as $Rb1^{F/F}$, $Rb1^{F/+}$, and $Rb1^{+/+}$ for simplicity (Supplementary Figure E1, online only, available at www.exphem.org).

Recombination was successful at the *Rb1* locus in B cells from $Rb1^{F/F}$ mice stimulated to undergo CSR ex vivo (Fig. 1B; Supplementary Figure E2, online only, available at www.exphem.org). Recombination was also detected in vivo in splenic GC cells ($B220^+GL7^+IgG1^+$)

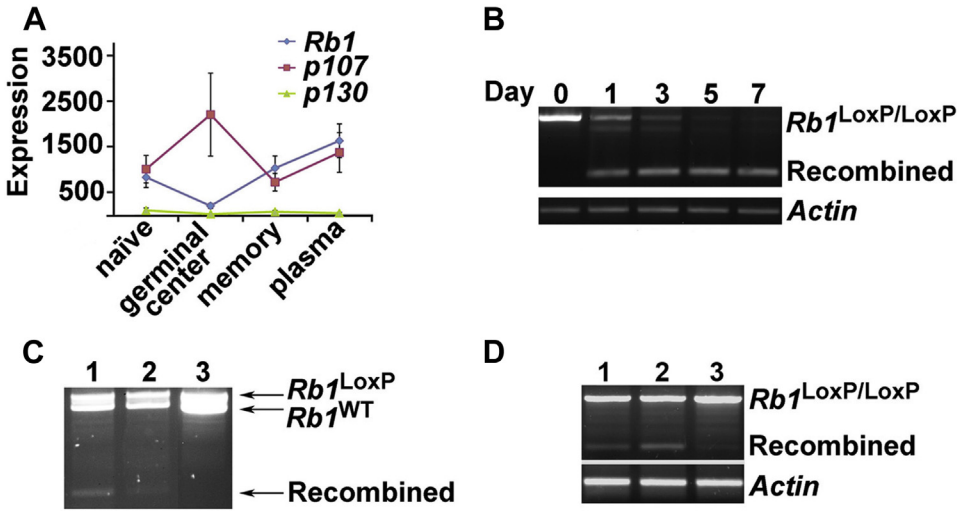

Figure 1. Generation of triple transgenic mice without *Rb1* gene function in GC B cells. (**A**) Pattern of expression of *Rb1* family members in mature B-cell subsets. mRNA microarray expression data (arbitrary units) of retinoblastoma family members *Rb1*, *p107*, and *p130* in flow-sorted primary late B-cell populations from wild-type mice [21]. (**B**) Polymerase chain reaction (PCR) analysis of DNA isolated from $Rb1^{F/F}$ mouse spleen B cells after ex vivo stimulation with IL-4 at the indicated time points (day 0 to day 7). *β-actin* was used as a loading control. (**C**) *Rb1* recombination in splenic B cells and bone marrow $CD138^+$ cells of $Rb1^{F/+}$ mouse after NP-CGG immunization by PCR. Lane 1: mouse spleen B-cells, lane 2: mouse bone marrow CD138+ cells, lane 3: mouse tail DNA, used as a negative control. (**D**) Recombination in a panel of cell types of $Rb1^{F/F}$ mouse after NP-CGG immunization by PCR. Lane 1: mouse bone marrow $B220^+IgM^-$cells (early B cells), lane 2: mouse spleen B cells, lane 3: bone marrow $B220^-Ly6G^+$ cells (granulocytes). *β-actin* is the loading control. (Color version of figure available online.)

and in post-GC plasma cells (B220$^-$, CD138$^+$) of *Rb1*$^{F/+}$ mice (Fig. 1C). Small amounts of recombination were detected in *Rb1*$^{F/F}$ bone marrow B cells, suggesting small amounts of off-target cre expression in pre-GC B cells. No recombination was detected in myeloid lineage cells (Fig. 1D). To address the off-target effects observed in the *Rb1*$^{F/F}$ mice, we mated *Rb1*$^{F/F}$ mice to AID-cre mice, which drive cre expression in GC cells undergoing CSR. These matings did not yield genotypes at expected mendelian frequencies, and we were unable to generate AID-Cre-*Rb1*$^{F/F}$-p107$^{-/-}$ mice. This was likely due to embryonic lethality, as AID is expressed in embryonic neuronal cells [23], and *Rb1* null mice are embryonic lethal because of neuronal defects [2,13,14].

We anticipated cell cycle deregulation in GC B cells with *Rb1* deficiency, so we measured proliferation in naive splenic B cells from our triple transgenic *Rb1*$^{+/+}$, *Rb1*$^{F/+}$, and *Rb1*$^{F/F}$ mice stimulated to undergo CSR ex vivo.

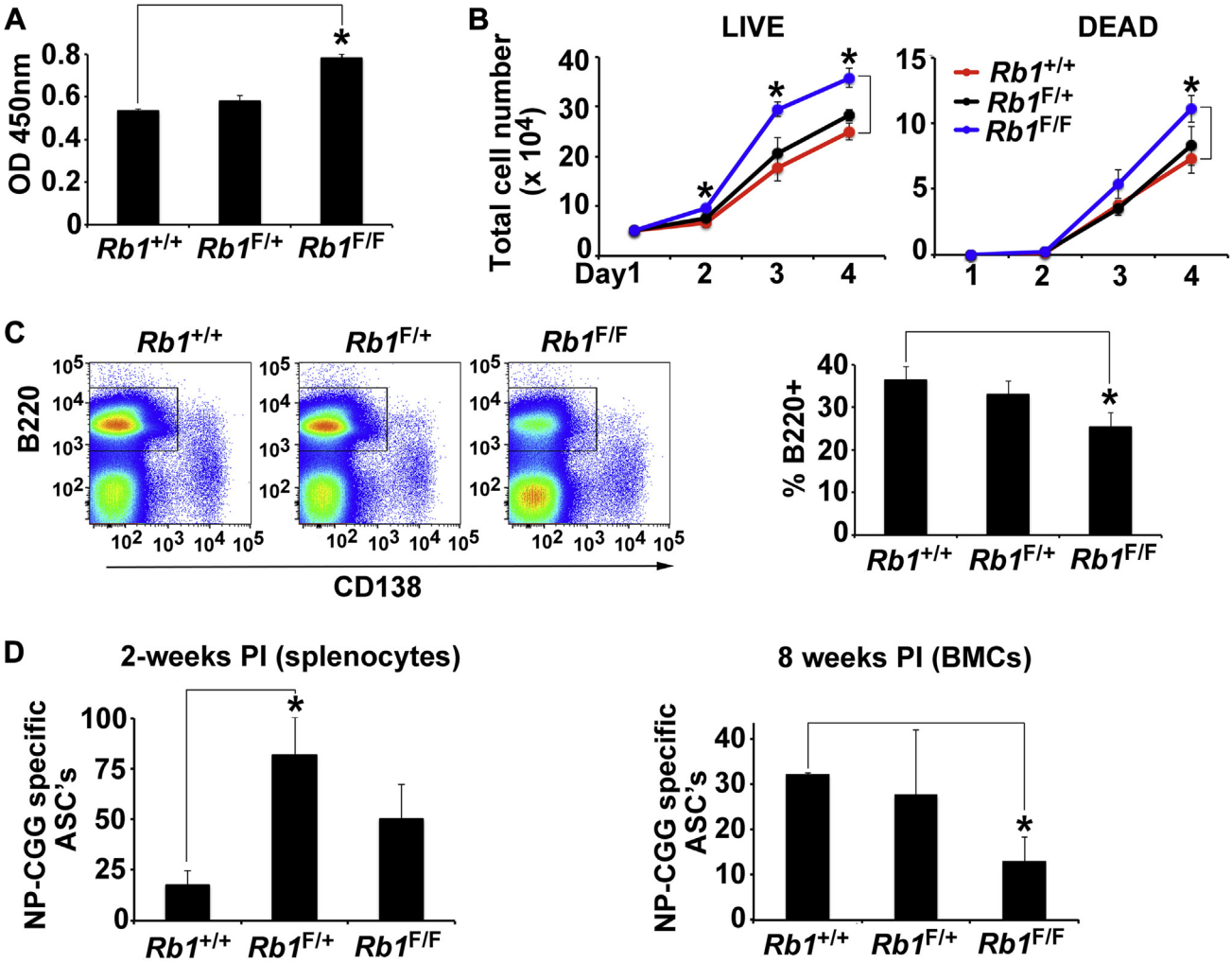

Figure 2. Hyperproliferation and cell death of B cells undergoing class-switch recombination. (**A**) Bromodeoxyuridine (BrdU) assay of splenic B cells isolated from *Rb1*$^{+/+}$, *Rb1*$^{F/+}$, and *Rb1*$^{F/F}$ triple transgenic mice stimulated with IL-4 and LPS for 3 days. Equal numbers of cells from each genotype were pulsed with BrdU, and the optical density (OD) at 450 nm was measured. The experiment was performed three times in quadruplicate; a representative analysis is shown. (**B**) Growth curves of splenic B cells derived from *Rb1*$^{+/+}$, *Rb1*$^{F/+}$, and *Rb1*$^{F/F}$ mice stimulated with IL-4 and LPS. Equal numbers of cells were plated in triplicate on day 1. Cells were counted each day for 3 days using trypan blue. Live cells (trypan blue excluded) are on the left, and dead cells (trypan blue stained) on the right. The experiment was performed three separate times in triplicate; a representative analysis is shown. (**C**) Flow cytometry analysis of splenic CD138$^+$B220$^-$ (plasma) cells of *Rb1*$^{+/+}$ and *Rb1*$^{F/F}$ triple transgenic mice 2 weeks after NP-CGG immunization (left). The average percentage of bone marrow B220$^+$ cells ($n = 6$ mice of each genotype) was analyzed on separate days (right). (**D**) ELISA-SPOT assays were performed 2 weeks post-immunization (PI) with NP-CGG on splenocytes (left) and 8 weeks PI on whole bone marrow cells (BMCs) isolated from *Rb1*$^{+/+}$, CG-*Rb1*$^{F/+}$, and *Rb1*$^{F/F}$ mice. NP-CGG-specific antigen-secreting cells (ASCs) were quantitated by counting spots (Methods). For the splenocyte analysis, ASCs per 400,000 plated cells in duplicate is shown ($n = 6$ mice per genotype). For the BMC analysis, percentages of ASCs per 460,000 plated cells in duplicate are illustrated. For *Rb1*$^{+/+}$, $n = 2$, and for *Rb1*$^{F/+}$ and *Rb1*$^{F/F}$, $n = 4$. For all experiments, error bars are SEM. Statistical analyses were performed using a two-tailed, unpaired *t* test. *$p < 0.05$.

Proliferation was significantly increased in $Rb1^{F/F}$ spleen cells compared with $Rb1^{+/+}$ controls assessed by both BrdU incorporation (Fig. 2A) and cell growth assays (Fig. 2B), although they did not proliferate past day 4 of culture (not shown), suggesting the cells were not transformed. We observed significantly more dead cells among $Rb1^{F/F}$ B cells (Fig. 2B). Our observation that *Rb1* deficiency in GC B cells caused both increased proliferation and cell death has been made in other cell types and is consistent with *Rb1*'s well-known function as a cell cycle checkpoint and apoptotic regulator [11].

To assess the effect of *Rb1* deficiency on GC B cells in vivo, we measured short-term GC splenic B-cell responses following immunization. Mice were stimulated with NP-CGG, and 2 weeks later, B-cell subsets were assessed by immunophenotyping using five-color flow cytometry. Despite the ex vivo proliferation we observed, no significant differences were observed in immature B cells (IgM^+ IgD^-), activated B cells (IgM^+ IgD^+), follicular cells (IgM^{low} IgD^+), GC B cells ($B220^+IgD^-GL7^+$, data not shown), or plasma cells ($B220^{-/low}$ $CD138^+$) (Fig. 2C). We did observe a decrease in the percentage of $B220^+$ splenocytes isolated from $Rb1^{F/F}$ mice compared with $Rb1^{+/+}$ control mice, suggesting that *Rb1* deficiency in early B cells may lead to increased apoptosis, but no differences were observed in the percentage of $B220^+CD138^+$ bone marrow plasma cells across the three mouse strains (Fig. 2C).

We next measured antigen-specific plasma cell responses using NP-CGG ELISA-SPOT assays and splenocytes from each of the three strains of mice. Unexpectedly, the $Rb1^{F/+}$ mice had an increase in splenic NP-CGG-specific ASCs compared with $Rb1^{+/+}$ controls, but the $Rb1^{F/F}$ mice did not. Following successful CSR in GCs, B cells differentiate to plasma cells and home to the bone marrow. To assess B-cell subsets at a later point (8 weeks post-immunization [PI]), we measured B and plasma cells in the bone marrow and spleen of the three mouse strains by measuring percentages of each by flow cytometry, as described above. We observed no significant changes in any of the B-cell subsets we tested (data not shown). To quantitate antigen-specific plasma cell responses, NP-CGG ELISA-SPOT assays were performed using bone marrow cells from each of the three strains of mice. $Rb1^{F/F}$ mice had significantly fewer NP-CGG ASCs compared with $Rb1^{+/+}$ mice, suggesting that loss of *Rb1* in post-GC B cells may induce cell death.

$Rb1^{F/+}$ and $Rb1^{F/F}$ mice developed normally and appeared healthy. To screen these mice for malignancy, we assessed an array of biomarkers when mice reached the age of 12 months after NP-CGG stimulation. Complete blood counts (CBCs) revealed that, compared with $Rb1^{F/+}$ and $Rb1^{+/+}$ mice, $Rb1^{F/F}$ mice had slightly, but not significantly increased white blood cell and lymphocyte counts (Supplementary Figure E3, online only, available at www.exphem.org). Serum protein electrophoresis (SPEP) analysis revealed no significant M-proteins in any of the mice (Supplementary Figure E4, online only, available at www.exphem.org). X-Ray analysis was used to detect lytic bone lesions, a hallmark of MM, but none were detected (Supplementary Figure E5, online only, available at www.exphem.org). No significant abnormalities were seen in vivo, as determined with chemistry tests (serum creatinine, calcium, blood urea nitrogen, albumin, and total protein) and histopathologic analysis of organs (heart, liver, lung, kidney, spleen—data not shown). These data suggest that no MM or other B-cell malignancy developed in $Rb1^{F/+}$ or $Rb1^{-/-}$ mice, within 12 months of follow-up.

Together our data indicate that *Rb1* function is essential for control of proliferation of GC B cells, but that loss of this tumor suppressor is not sufficient to initiate malignant transformation. Rather, B-cell numbers were decreased in the absence of *Rb1* (Fig. 2). The C-γ-driven Cre expression predicts recombination in GC B cells; however, we detected "off-target" recombination in bone marrow B cells (Fig. 1). We also observed fewer NP-CGG-specific BM ASCs in $Rb1^{F/F}$ mice. These results may be explained by the fact that E2F factors activated by *Rb1* loss induce apoptosis through p53 in certain cell types [24]. This is consistent with the observation that although haplo-insufficiency for *RB1* is common, complete loss of *RB1* is rare in the absence of other mutations to protect the cells from death.

Additional mutations are required to cooperate with *Rb1* loss for malignant transformation of GC B cells. Our finding that GC B cells haplo-insufficient for *Rb1* hyperproliferate in response to antigen stimulation (Fig. 2) suggests that malignant cells may optimize the *Rb1* dose for best proliferative advantage. This would provide an explanation for the frequent mono-allelic *RB1* loss and rare homozygous deletion in MM. Although *RB1* is affected by microdeletions and point mutations [4], large deletions affecting 13q are far more common in MM. Large deletions may facilitate MM growth and survival by simultaneously reducing the expression of *RB1* and another 13q gene or genes. One such candidate is *DIS3*, a 3′-to-5′ RNA exonuclease recurrently mutated in MM and located at chromosome 13q22.1. Notably, *DIS3* mutations detected in MM reduce, but do not eliminate, DIS3 activity. Hypomorphic DIS3 dysregulates the cell cycle through a mechanism that increases centromeric RNA and modification of chromatin structures near centromeres (unpublished data). Our mouse model will be a useful reagent for exploring the role of cooperation between *Rb1* loss and reduced Dis3 activity and testing the role of *Rb1* loss and MM-associated gain-of-function oncogene mutations.

Acknowledgments

This work was supported by the Barnes Hospital Foundation (MHT) and NIH Grant R01 CA175349 (MHT). The funders had no role in study design, data collection and analysis, decision to publish, or preparation of the article.

The authors thank members of the Tomasson lab for critical review of the article. We thank the Michael Dyer lab for providing the *Rb1*$^{LoxP/LoxP}$ and *p107*$^{-/-}$ mouse strains and the Stefano Casola lab for providing the c-gamma-1 cre mouse strain. We thank Dr. Deborah Novack for the pathology analysis. The Siteman Flow Cytometry Core Musculoskeletal Histology Core and Developmental Biology Histology Core provided excellent technical assistance.

Author contributions

ZH, JO, WCW, and NM designed and performed experiments. JL, YH, and MYS performed experiments. ZH and JO wrote the article. MHT designed the experiments and wrote the article.

Conflict of interest disclosure

The authors have no conflicts to disclose.

References

1. Zojer N, Konigsberg R, Ackermann J, et al. Deletion of 13q14 remains an independent adverse prognostic variable in multiple myeloma despite its frequent detection by interphase fluorescence in situ hybridization. Blood. 2000;95:1925–1930.
2. Vooijs M, Berns A. Developmental defects and tumor predisposition in Rb mutant mice. Oncogene. 1999;18:5293–5303.
3. Dao DD, Sawyer JR, Epstein J, et al. Deletion of the retinoblastoma gene in multiple myeloma. Leukemia. 1994;8:1280–1284.
4. O'Neal J, Gao F, Hassan A, et al. Neurobeachin (NBEA) is a target of recurrent interstitial deletions at 13q13 in patients with MGUS and multiple myeloma. Exp Hematol. 2009;37:234–244.
5. Walker BA, Leone PE, Jenner MW, et al. Integration of global SNP-based mapping and expression arrays reveals key regions, mechanisms, and genes important in the pathogenesis of multiple myeloma. Blood. 2006;108:1733–1743.
6. Chapman MA, Lawrence MS, Keats JJ, et al. Initial genome sequencing and analysis of multiple myeloma. Nature. 2011;471:467–472.
7. Egan JB, Shi CX, Tembe W, et al. Whole-genome sequencing of multiple myeloma from diagnosis to plasma cell leukemia reveals genomic initiating events, evolution, and clonal tides. Blood. 2012;120:1060–1066.
8. Zandecki M, Facon T, Preudhomme C, et al. The retinoblastoma gene (RB-1) status in multiple myeloma: A report on 35 cases. Leuk Lymphoma. 1995;18:497–503.
9. Juge-Morineau N, Harousseau JL, Amiot M, Bataille R. The retinoblastoma susceptibility gene RB-1 in multiple myeloma. Leuk Lymphoma. 1997;24:229–237.
10. Juge-Morineau N, Mellerin MP, Francois S, et al. High incidence of deletions but infrequent inactivation of the retinoblastoma gene in human myeloma cells. Br J Haematol. 1995;91:664–667.
11. Burkhart DL, Sage J. Cellular mechanisms of tumour suppression by the retinoblastoma gene. Nat Rev Cancer. 2008;8:671–682.
12. Classon M, Harlow E. The retinoblastoma tumour suppressor in development and cancer. Nat Rev Cancer. 2002;2:910–917.
13. Jacks T, Fazeli A, Schmitt EM, et al. Effects of an Rb mutation in the mouse. Nature. 1992;359:295–300.
14. Lee EY, Chang CY, Hu N, et al. Mice deficient for Rb are nonviable and show defects in neurogenesis and haematopoiesis. Nature. 1992;359:288–294.
15. Sage J, Miller AL, Perez-Mancera PA, Wysocki JM, Jacks T. Acute mutation of retinoblastoma gene function is sufficient for cell cycle re-entry. Nature. 2003;424:223–228.
16. Vooijs M, van der Valk M, te Riele H, Berns A. Flp-mediated tissue-specific inactivation of the retinoblastoma tumor suppressor gene in the mouse. Oncogene. 1998;17:1–12.
17. Dannenberg JH, Schuijff L, Dekker M, van der Valk M, te Riele H. Tissue-specific tumor suppressor activity of retinoblastoma gene homologs p107 and p130. Genes Dev. 2004;18:2952–2962.
18. Lee MH, Williams BO, Mulligan G, et al. Targeted disruption of p107: functional overlap between p107 and Rb. Genes Dev. 1996;10:1621–1632.
19. Robanus-Maandag E, Dekker M, van der Valk M, et al. p107 is a suppressor of retinoblastoma development in pRb-deficient mice. Genes Dev. 1998;12:1599–1609.
20. Sage J, Mulligan GJ, Attardi LD, et al. Targeted disruption of the three Rb-related genes leads to loss of G(1) control and immortalization. Genes Dev. 2000;14:3037–3050.
21. Bhattacharya D, Cheah MT, Franco CB, et al. Transcriptional profiling of antigen-dependent murine B cell differentiation and memory formation. J Immunol. 2007;179:6808–6819.
22. Casola S, Cattoretti G, Uyttersprot N, et al. Tracking germinal center B cells expressing germ-line immunoglobulin gamma1 transcripts by conditional gene targeting. Proc Natl Acad Sci USA. 2006;103:7396–7401.
23. Rommel PC, Bosque D, Gitlin AD, et al. Fate mapping for activation-induced cytidine deaminase (AID) marks non-lymphoid cells during mouse development. PLoS One. 2013;8:e69208.
24. Polager S, Ginsberg D. E2F—At the crossroads of life and death. Trends Cell Biol. 2008;18:528–535.

Supplementary data

Methods

Mouse models

To establish CG-Rb1F/F-p107$^{-/-}$, CG-Rb1F/+-p107$^{-/-}$, and CG-Rb1WT-p107$^{-/-}$ mouse models that conditionally delete Rb1 in spleen germinal center B cells, we generated strains of mice by breeding Rb1Flox/Flox mice to the Rb family member, p107$^{-/-}$ mice. Rb1Flox/Flox-p107$^{-/-}$ mice were bred to the germinal center-specific Cγ1-Cre mice that have the Cre recombinase knocked into the endogenous Cγ1 locus, which is expressed specifically during B-cell class-switch recombination. Rb1F/F and p107$^{-/-}$ mice were backcrossed 10 times to C57BL/6J. The p107$^{-/-}$ mice retained their brown color-likely because the Agouti genes are relatively close on chromosome 2 to p107. The CG mice were on a C57BL/6J background when obtained. Rb1 locus recombination was tested by polymerase chain reaction, as previously described [2]. Products obtained from Rb1LoxP alleles were 780 bp, and those from Rb1WT alleles were 680 bp. Recombined alleles were 260 bp. At 6 weeks of age, all mice were immunized using 1 mg of (4-hydroxy-3-nitrophenyl) acetyl-conjugated chicken γ-globulin (NP-CGG; Biosearch Technologies), which was mixed with Freund's Adjuvant Complete or Incomplete (Sigma-Aldrich) for primary or boosting immunization in 100 μL to inject intraperitoneally to promote germinal center B-cell activation and Rb1 conditional deletion. All mice were maintained under specific pathogen-free conditions and used according to institutional guidelines.

Ex vivo class-switch recombination assay

Murine splenocytes were treated with red blood cell lysing buffer (Sigma), and B cells were isolated using CD43 magnetic bead depletion (LD) columns (Miltenyi) Biotech with an AutoMacs Pro separator according to the manufacturer's instructions. Splenic B cells were cultured with 20 ng/mL interleukin (IL)-4 (R&D Systems, Minneapolis, MN) and 10 μg/mL lipopolysaccharide (LPS, Sigma-Aldrich) in B-cell medium (RPMI-1640) with L-glutamine (Cellgro, Manassas, VA), 1% HEPES, 1% penicillin/streptomycin/amphotericin B, 10% fetal bovine serum (Hyclone, South Logan, UT) for the indicated times.

Immunophenotyping by flow cytometry

Spleens and bone marrow were harvested from mice, passed through 50-μm CellTrics filters (Partec) to generate single-cell suspensions, and briefly treated with hypotonic lysis buffer to remove red blood cells. Cells (10×10^6) were then suspended in 0.5 mL staining buffer (phosphate-buffered saline, 0.5% bovine serum albumin, 0.05% NaN_3) and incubated with the following rat anti-mouse monoclonal antibodies (all purchased from BD Biosciences unless indicated otherwise) in the dark on ice for 30 min: APC-Cy7 B220 (RA3-6B2), Brilliant Violet 421 CD138 (281-2), PE GL7 (GL7), FITC IgM (II/41), and PerCP-Cy5.5 IgD (11-26c.2a, BioLegend). Cells were then washed twice with staining buffer and resuspended in 0.5 mL; flow cytometric analysis was performed on a FACScan (Becton Dickinson), modified with additional lasers (Cytek Development). A total of 1×10^6 events were collected. FlowJo software (Tree Star) was used for data analysis.

Cell proliferation (BrdU and cell counting)

For bromodeoxyuridine (BrdU) assays, IL-4- and LPS-treated B cells were cultured (as described above) for 3 days. On the third day, proliferation was tested by pulsing 25,000 cells of each genotype with BrdU for 2 hours using an ELISA BrdU Kit (Cell Signaling) according to the manufacturer's instructions. For cell counting, 50,000 cells were plated for each genotype in triplicate on day 1. Viable cells were counted using trypan blue exclusion; cells that had taken up the dye were considered dead and also counted. Cells were counted on a hemocytometer.

ELISA-SPOT assays

MultiScreen nitrocellulose filter plates (EMD Millipore) were coated with 50 μg/mL NP16-BSA (Biosearch Technologies) or BSA alone as a control and incubated overnight at 4°C. Splenocytes (2 weeks postimmunization) or bone marrow cells (8 weeks postimmunization) were seeded at decreasing doses in duplicate. Cells were cultured in 100 μL overnight at 37°C, 5% CO_2. Wells were washed with PBS with 0.5% Tween and stained with biotinylated anti-mouse IgG. Plates were washed and next incubated with streptavidin-conjugated horseradish peroxidase (BD Pharmingen). Spots were developed using 3-amino-9-ethyl-carbazole (Sigma). Once spots appeared, the reaction was quenched by rinsing wells with water. Spots were counted using an ImmunoSpot S6 Analyzer (CTL Laboratories).

Complete blood count analysis

The complete blood count (CBC) was quantitated using the HEMA VET 950 system (Drew Scientific, Dallas, TX).

Serum protein electrophoresis analysis

Serum samples were analyzed by serum protein electrophoresis (SPEP) analysis on a Quickgel Chamber apparatus using precasted quickGels (Helena Laboratories) according to the manufacturer's instructions. Densitometric analysis of the SPEP traces was performed using the clinically certified Helena QuickScan 2000 workstation.

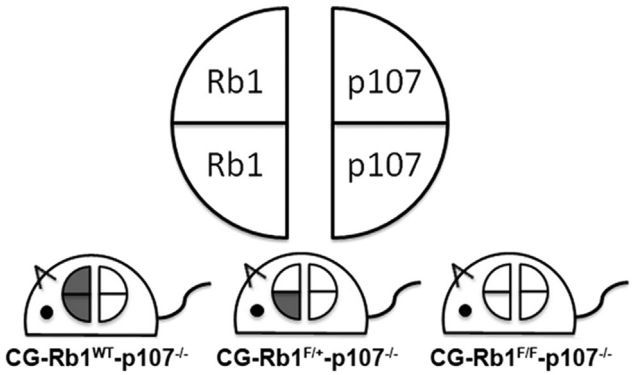

Supplementary Figure E1. Schematic of the three mouse strains.

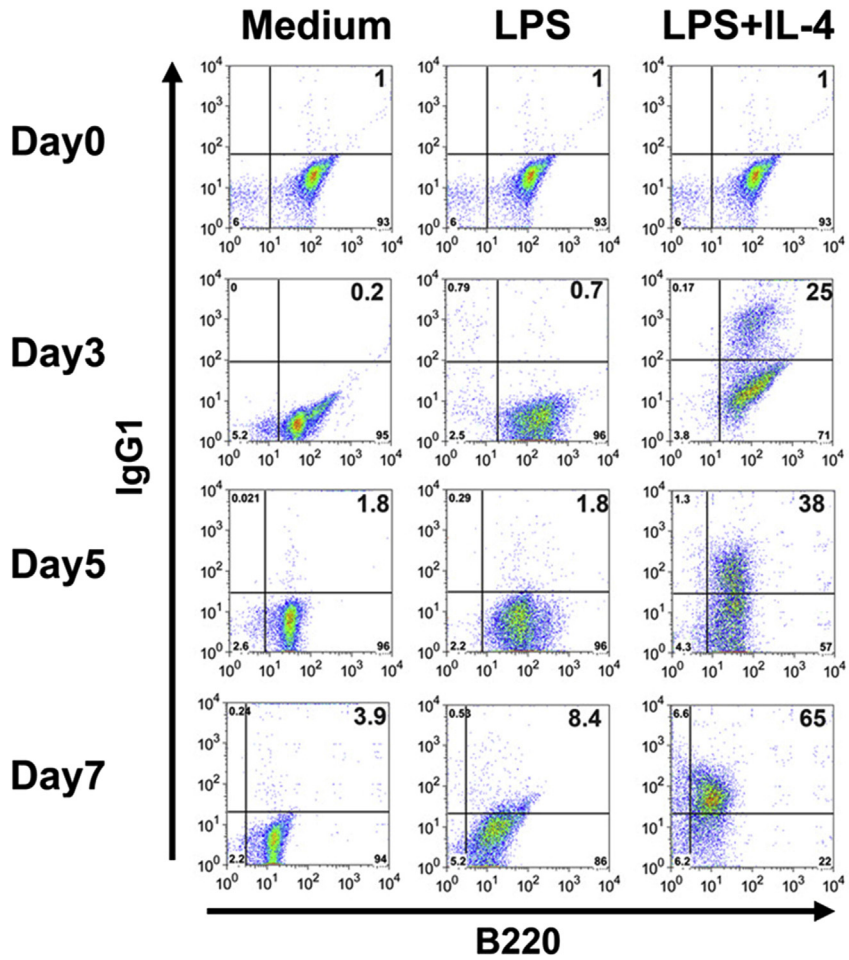

Supplementary Figure E2. Ex vivo class switching of primary murine B cells and Cre-mediated recombination. Flow cytometery was used to measure the IgG1 levels of CG-Rb1F/FP107$^{-/-}$ splenic B cells after ex vivo class-switch recombination with medium only, LPS only, or LPS plus IL-4, at different time points.

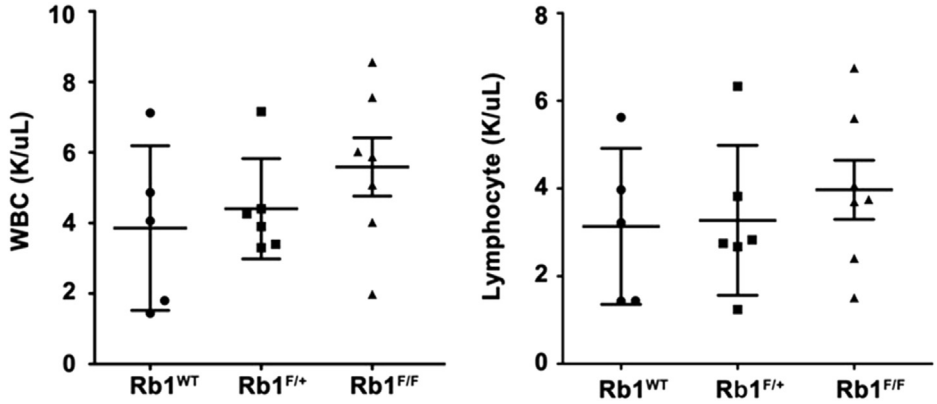

Supplementary Figure E3. Mouse blood cell counts 12 months after immunization. Total white blood cell counts (left) and lymphocyte counts (right) of peripheral blood from the three mouse strains at the age of 12 months: CG-Rb1^{WT}-p107$^{-/-}$ ($n = 5$), CG-Rb1$^{F/+}$-p107$^{-/-}$ ($n = 6$) and CG-Rb1F/^{F}–p107$^{-/-}$ ($n = 6$) after NP-CGG immunization at the age of 6 weeks.

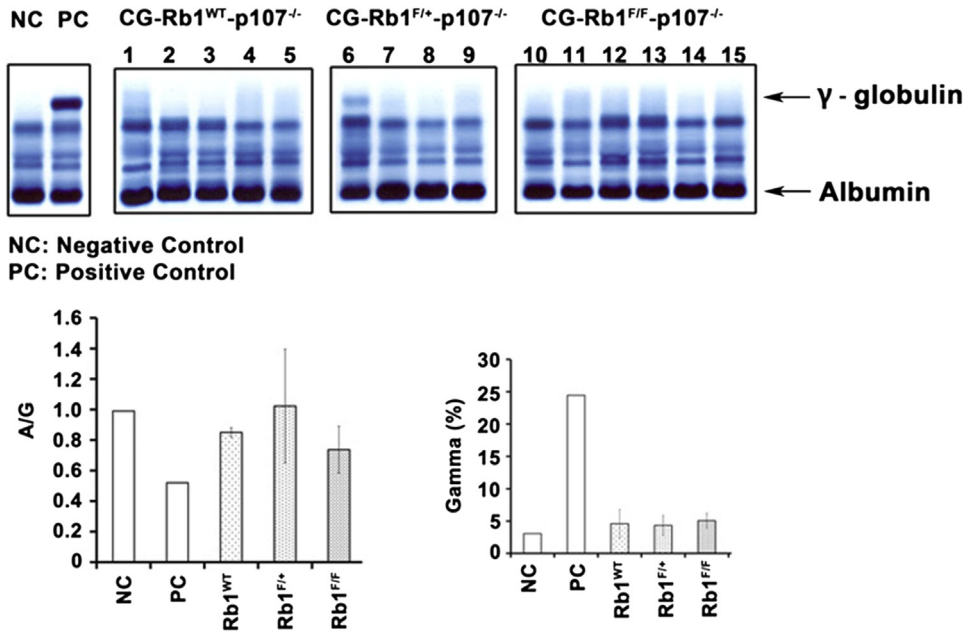

Supplementary Figure E4. Detection of M-protein bands by serum protein electrophoresis (SPEP). Top: SPEP gels for the three mouse strains. CG-Rb1WTP107$^{-/-}$ (lanes 1–5), CG-Rb1$^{F/+}$P107$^{-/-}$ (lanes 6–9), CG-Rb1$^{F/F}$P107$^{-/-}$ (lanes 10–15). NP = negative control, PC = positive control. The *arrows* point to the γ-globulin and albumin bands. Bottom: SPEP albumin/globulin (A/G) ratios for the different strains of mice (left) and SPEP gamma (γ) fractions (percentage of gamma fraction in total serum protein) for the three mouse strains.

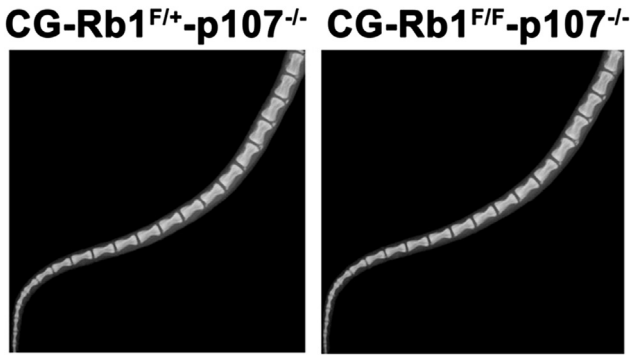

Supplementary Figure E5. Radiograph of mouse tails at the age of 12 months.